Langmuir

ARTICLE

pubs.acs.org/Langmuir

Label-Free Raman Mapping of Surface Distribution of Protein A and IgG Biomolecules

Zachary A. Combs, Sehoon Chang, Tolecia Clark, Srikanth Singamaneni, Kyle D. Anderson, and Vladimir V. Tsukruk*

School of Materials Science and Engineering, Georgia Institute of Technology, Atlanta, Georgia, United States

ABSTRACT: We have demonstrated a nanoengineered substrate composed of micropatterned silver nanoparticles to be used for the label-free mapping of adsorbed biomolecules. We utilized surface-enhanced Raman scattering (SERS) phenomenon to monitor the known bioanalytes, protein A and human immunoglobulin G (IgG). The SERS substrate was composed of a poly(alylamine hydrochloride) (PAH)/poly(styrenesulfonate) (PSS) layer-by-layer (LbL) nanocoating micropatterned with silver nanoparticles confined to microscopic stripes. Selective adsorption of biomacromolecules is facilitated by the amine-terminated LbL nanocoating, which prevents the surface adsorption of positively charged protein A across the surface except on the patterned regions containing negatively charged silver nanoparticles. Furthermore, adsorption of IgG on predetermined regions is facilitated by the selective binding of the Fc region of IgG to protein A. This label-free SERS approach provides accurate, selective, and fast detection of protein A and IgG solutions with a nanomolar concentration, down to below 1 nM for IgG in solution. This method could also be utilized for the facile detection of proteins in field conditions as well as in clinical, forensic, industrial, and environmental laboratories.

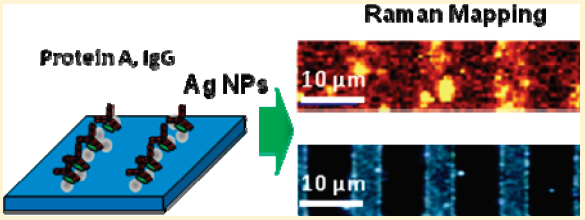

INTRODUCTION

Biosensing devices are designed to specifically bind selected biomolecules and subsequently convert this local event to a measurable signal.[1] The mechanism of biomolecular detection is frequently based on measuring specific optical absorption such as that implemented in the enzyme-linked immunosorbent assay (ELISA) method,[2] surface plasmon resonance (SPR) techniques,[3] or fluorescence resonance energy transfer (FRET).[4] These well-known methods, however, do not provide a ready pathway for facile and direct label-free detection of the biomolecular analytes within one measuring cycle. These approaches often require a complex sequence of synthesis of labeled molecules and specimen preparation, which are costly and time-consuming, rely on synthetic routines that might or might not work for selected biomolecules, and must be designed specifically for the biomolecular system of interest. This novel, rapid, and simple method for the label-free trace detection of selected proteins has clear advantages such as no complicated sample preparation or multiple intermediate steps that facilitate "user-friendly" and relatively universal biosensing routines. In addition, such a facile routine should improve the range of prospective applications, limiting sensitivity, and accuracy of detection for future biosensing approaches.

Among numerous methods of biodetection, surface-enhanced Raman scattering (SERS) has become an area of intense research as a highly sensitive probe for trace level detection of small molecules since the demonstration of single molecule detection.[5−7] The highly sensitive vibrational spectroscopic technique of SERS can potentially provide a method for label-free sensing and analysis of proteins, down to single molecules, which was previously impossible due to the complexity of such biomolecules.[8−11] To realize potential advantages of this approach, there have been various suggested designs to provide dramatic enhancement for the SERS response. The SERS phenomenon is possible due to the large electromagnetic fields that exist in the small gaps between metal nanostructures called hot spots.[12] The design of the substrate on which the SERS phenomenon becomes significant is the most critical aspect of a sensitive biomolecular probe.[13] Most popular designs involved various engineered substrates such as roughened metal nanoparticle films,[14,15] metallic and bimetallic nanostructures,[16−19] and 3D porous substrates.[20]

Among important biological molecules, IgG is the most abundant immunoglobulin in the blood and is produced in large quantities during secondary immune responses.[21] The binding of the Fc region of IgG, which coats microorganisms in the blood, and the Fc receptors of macrophages and neutrophils allows these phagocytic cells to bind, ingest, and destroy invading bacteria.[22] The accurate and trace detection of IgG is extremely important in an effort to better understand its role in complement responses in the body and other concentration dependent roles it may play, as well as provide a precedent for the label-free detection of other biomolecules. Standard fluorescent-based methods for IgG detection, such as ELISA, are widely used, but these methods have certain drawbacks such as photobleaching, time-consuming sample preparation, and a moderate limit of analyte detection.[23] Previous SERS studies have been performed for IgG,[24,25] leading to a characteristic spectrum of this biomolecule. These studies, however, show a range of peaks that are

Received: December 1, 2010
Revised: December 20, 2010
Published: February 04, 2011

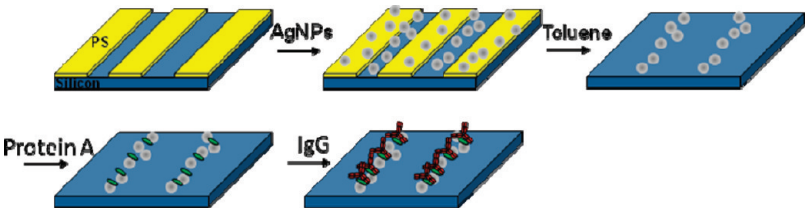

Figure 1. Fabrication steps of the micropatterned SERS substrate with silver nanoparticles and subsequent binding of protein A and IgG. The striped pattern of silver nanoparticles was made via the capillary transfer lithography technique.[30]

likely caused by complex enhancement, which depends upon the orientation of the polarizable component of the vibration with respect to the metal surface.[26,27]

To facilitate highly sensitive detection of trace amounts of biomolecules and separate numerous secondary contributions, a new substrate must be designed to allow selective adsorption of proteins in active regions, thus increasing the selectivity and level of detection and providing concurrently measured background for nonselectively adsorbed compounds under identical conditions.[28] Micropatterned surfaces are frequently used as SERS substrates due to their high degree of order, simplicity of microstamping fabrication, and reproducible results, which cannot be provided by other surfaces.[29,30] Soft lithography is a simple process that can be adopted to fabricate micropatterned arrays for selective adsorption.[31] Micron-sized, long-range ordered metal nanoparticle arrays extended over centimeter scale areas can be fabricated utilizing capillary transfer lithography.[32]

The high degree of order provided by micropatterned surfaces is critically important for separating the SERS-enhanced spectra of the biomolecule of interest and any background from the substrate and nonspecifically adsorbed species. These surfaces also provide the researcher with the ability to easily tailor the pattern to the specific system being studied. Other advantages of the micropatterned substrate are the ease of position control when measurements are taken and the elimination of common difficulties in background subtraction due to the simultaneous analyte and background measurements. The micropatterned surface allows for more reliable detection of very small concentrations of biomolecules due to identical collection conditions for signal and background and thus more accurate subtraction of substrate background, which might reach 50% at the lowest concentrations. Collecting background spectra for surface areas from other specimens in a separate experimental cycle dramatically compromises the quality of the background removal and thus the overall sensitivity of the procedure at the lowest concentrations.

In this study, we report on the rapid, label-free mapping of two selected biomolecules, protein A and IgG, adsorbed on a novel micropatterned SERS substrate down for nanomolar concentrations of solutions. The model system exploited in this study is the well-known binding reaction of protein A to the Fc region of IgG.[33] The substrate design suggested here provides a simple method that is much faster (less than several minutes of total experiment time) than current optical methods.

EXPERIMENTAL SECTION

Silver Nanoparticle Synthesis. Silver nanoparticles were synthesized by the photoreduction of $AgNO_3$ in the presence of sodium citrate by irradiation with ultraviolet light at room temperature producing monodisperse 33 ± 5 nm silver nanoparticles.[34] $AgNO_3$ (42.5 mg) and sodium citrate (73.5 mg) were dissolved in 250 mL of Nanopure water (18 MΩ cm), and an ultraviolet lamp (λ = 365 nm) was used as the light source for the reduction process with an exposure time of 8 h.

Micropatterned Substrate Fabrication. A micropatterned silver nanoparticle substrate was prepared using capillary transfer lithography over a 5 mm × 5 mm area. A simple diagram illustrating the soft lithography process exploited here is shown in Figure 1. Three bilayers of poly (allylamine hydrochloride) (PAH) (M_w = 70 000)/poly(styrenesulfonate) (PSS) (M_w = 70 000) and one more layer of PAH were deposited on a silicon substrate according to the standard procedure used in our lab.[35] [100] silicon substrates (Semiconductor Processing) with a native silicon oxide layer with 1.6 nm thickness were cleaned with piranha solution (3:1 concentrated sulfuric acid and hydrogen peroxide mixture; ***Caution!*** Piranha solution reacts violently with organic matter and should be handled with extreme care), abundantly rinsed with Nanopure water, and dried with dry nitrogen stream in accordance with the usual procedure.[36] They served as hydrophilic substrates for spin-assisted LbL film depositions of prelayers with uniform coverage over the whole surface area.[37,38]

A 400 nm thick polystyrene (PS) pattern with a periodicity of 10 μm defined by a poly(dimethylsiloxane) (PDMS) stamp was then deposited onto the LbL nanocoating. After patterning, silver nanoparticles were deposited on the patterned surface and the PS pattern was dissolved in toluene leaving striped regions of silver nanoparticles similar to the routine reported earlier.[39,40]

Optical and Fluorescent Microscopy and Ellipsometry. The striped pattern of silver nanoparticles was confirmed by optical microscopy operating in the dark field mode (Leica DM4000M). Utilizing the optical microscope in the fluorescent mode, we collected a fluorescent field image of fluorescein-labeled protein A on the silver nanoparticle array and a fluorescent field image of rhodamine-labeled IgG on a silver nanoparticle array. Both fluorophore-conjugated and unconjugated protein A and IgG were purchased from Rockland Immunochemicals and used as received. The substrate was exposed to a 10^{-6} M protein A solution and a 0.5 × 10^{-6} M IgG solution for 30 s each and washed thoroughly with Nanopure water between each solution exposure for preliminary studies. Effective thicknesses were obtained with M-2000U spectroscopic Ellipsometer (Woolam).

UV−Vis and Fluorescent Spectroscopy. UV−vis spectra of the nanoparticles in solution were recorded in 1.5 semimicro plastic cuvettes (PlastiBrand, Germany) using a UV-2450 spectrophotometer (Shimadzu). UV−vis spectroscopy of the micropatterned surface was completed using a Craic QDI 202 microscope spectrophotometer attached to Leica microscope with a 50× objective. Fluorescence spectra of the silver nanoparticle-micropatterned samples following fluorescein-conjugated protein A and rhodamine-conjugated IgG adsorption were recorded on a RF-5301PC spectrofluorophotometer (Shimadzu).

AFM Studies. Atomic force microscopy (AFM) scanning with a Dimension 3000-Nanoscope IIIa microscope of the silver nanoparticle array before and after protein A and IgG deposition was conducted with a rate of 0.5−1.0 Hz for surface areas of 50 μm × 50 and 20 μm × 20 μm according to usual procedure adapted in our lab.[41,42] Silicon nitride tips were used with tip radii of about 10 nm and spring constants of 42 N m^{-1}. High resolution AFM was performed with a Dimension

Multimode-Nanoscope IIIa, for scans of 500 nm × 500 nm areas in an enclosed chamber kept at less than 2% relative humidity. The AFM images of several different areas of the sample were collected and representative images were selected.

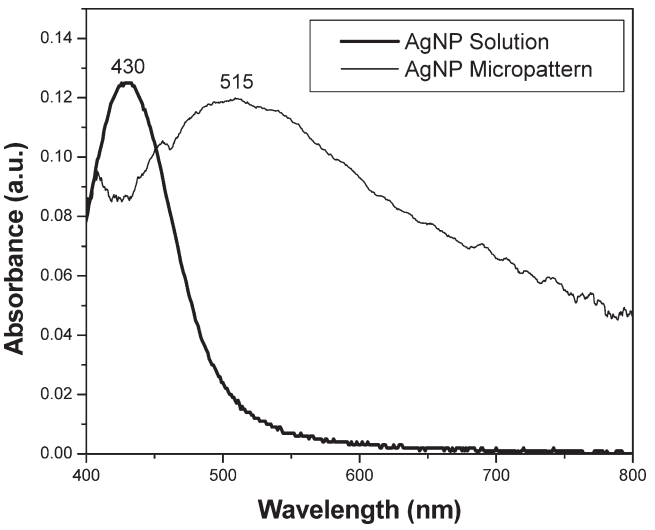

Figure 2. UV−vis spectra of the silver nanoparticles in solution and after aggregation on the micropatterned substrate.

Raman Studies. For the detection of protein A and IgG on the SERS array, a confocal Raman microscope (Alpha 300 R) (WITec) with a 514 nm Nd:YAG laser was employed as the incident light beam.[43] The image was acquired line by line with an Avalanche photodiode detector (APD) in the single photon counting mode by fast imaging with lateral resolution of ~500 nm and vertical resolution of 1 μm with a 50× objective lens. For detection limit studies, the SERS substrate was exposed to protein solutions with a series of concentrations down to a 10^{-10} M for 30 s each and washed thoroughly with Nanopure water before collections of Raman spectra.

RESULTS AND DISCUSSION

Nanoparticle and Substrate Characterization. The soft lithography technique used to fabricate the micropatterned susbstrate is shown in the schematic in Figure 1. The UV−vis absorption spectra of the particles before and after adsorption on the micropatterned surface are shown in Figure 2. The silver nanoparticles synthesized here show a strong absorption band at 430 nm, which is expected for nonaggregated silver nanoparticles with a citrate shell.[34] The position of the absorption band corresponds to nanoparticles of about 35 nm in diameter.[44] Upon adsorption and aggregation on the surface of the micropatterned substrate, the plasmon band shifts to a longer wavelength, which

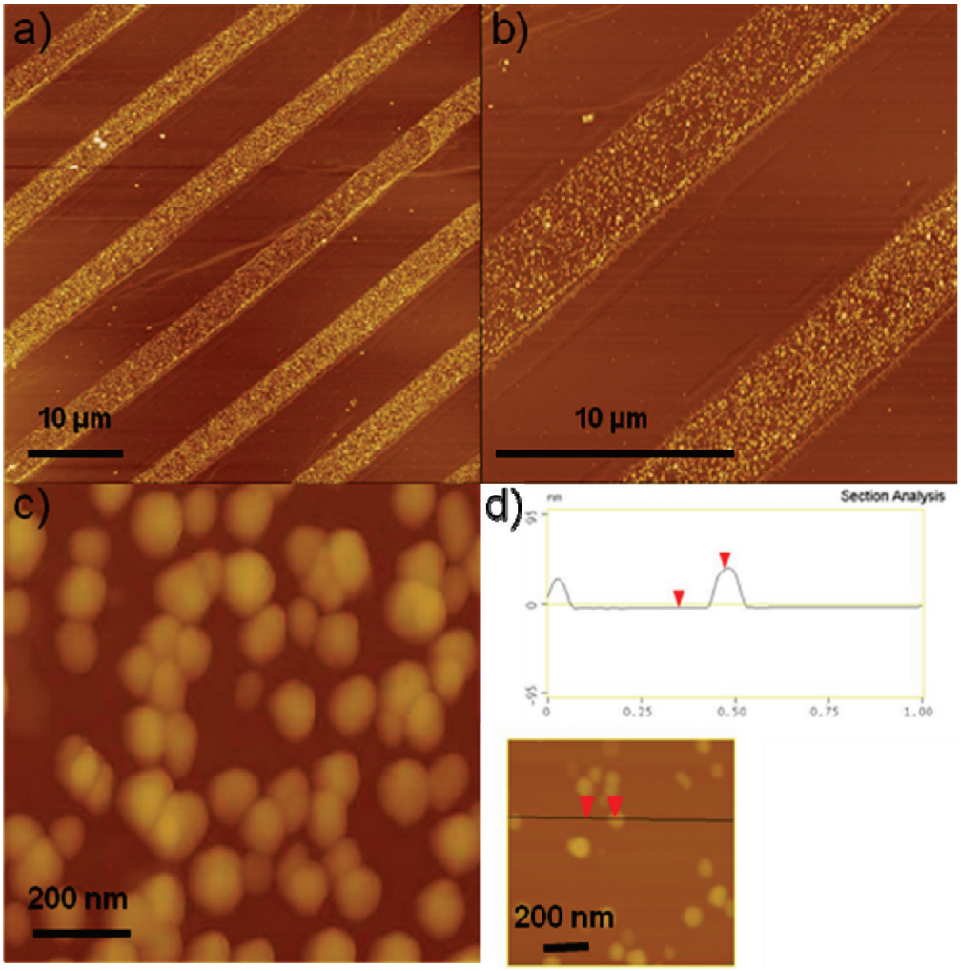

Figure 3. AFM topographical images of the micropatterned substrate with (a) 50 μm × 50 μm, (b) 20 μm × 20 μm, and (c) 1 μm × 1 μm scan sizes, and (d) a cross-section of individual nanoparticles. The z scale of all images is 200 nm.

dx.doi.org/10.1021/la104787w |*Langmuir* 2011, 27, 3198–3205

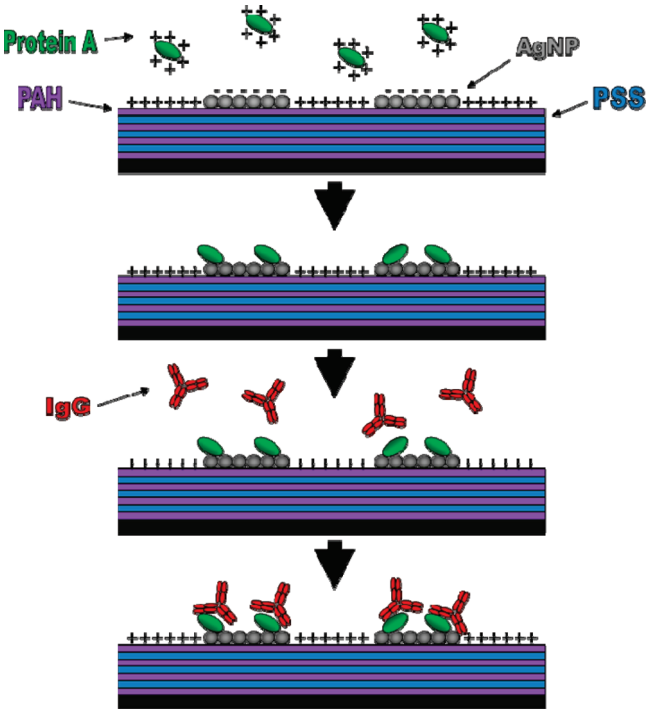

Figure 4. Diagram illustrating suggested sequential adsorption of protein A and IgG to the silver nanoparticle micropatterned SERS substrate.

is close to the wavelength of the laser used for the SERS measurements (514 nm), maximizing the SERS enhancement. The red shift of the silver nanoparticle plasmon band is a result of the coupling of the surface plasmons of the individual nanoparticles upon aggregation and has been well-documented in previous studies.[45−47]

AFM scanning confirmed highly selective adsorption of silver nanoparticles on amine-terminated areas (Figure 3a,b). The optimal concentration of AgNPs adsorbed on the patterned substrated was determine by sequential deposition cycles of AgNPs from solution. The maximum SERS intensity was seen at approximately 60% surface coverage. Further deposition cycles of AgNPs resulted in nonuniform multilayers of nanoparticles with no further SERS intensity increase. To further characterize the diameter of silver nanoparticles, high resolution AFM was completed for selected surface areas with uniform nanoparticle distribution within selected striped areas (Figure 3c). Cross sections through individual nanoparticles revealed an average diameter of 33 ± 5 nm, which corresponds closely to that suggested from the position of absorption band in UV−vis spectra (Figure 3d).

Patterning of Protein A and IgG. As introduced above, the different surface elements of the SERS substrate were designed to allow selective adsorption of protein A on regions of the patterned surface containing silver nanoparticles (Figure 4). The robust and uniform amine-terminated LBL nanocoating contributed to the specific adsorption of protein A on the SERS-active silver nanoparticles by preventing nonspecific adsorption through electrostatic repulsion. As expected, IgG should subsequently bind to the substrate only on selected surface regions by the well-documented specific binding of protein A to the Fc region of IgG (Figure 4). The adsorption of protein A was conducted at pH 5 where protein A exists as a more positively

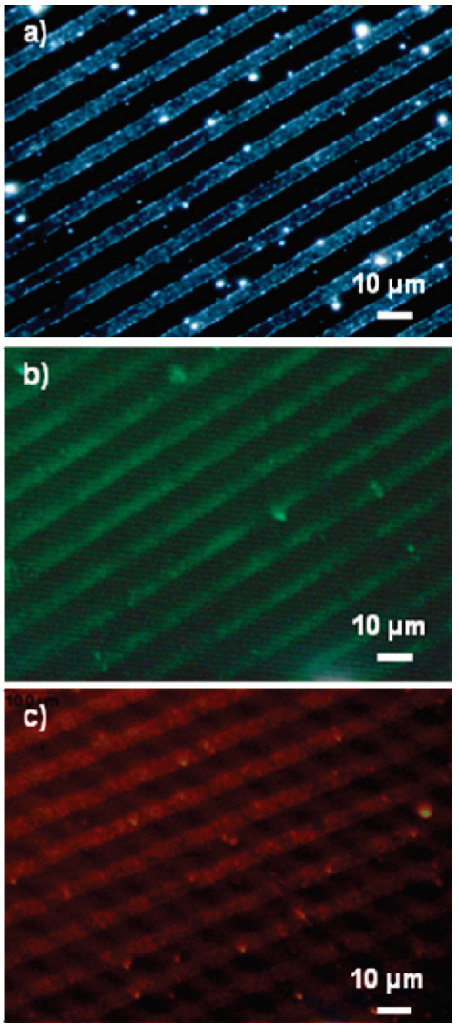

Figure 5. Fluorescent microscopy images of the silver nanoparticle micropatterned substrates (a) dark field before protein adsorption, (b) after fluorescein-conjugated protein A adsorption, and (c) after Rhodamine-conjugated IgG adsorption.

charged species.[48] The pH for the adsorption of IgG was increased to pH 7 to prevent any electrostatic repulsion between protein A and IgG which can occur at low pH where both molecules are more positively charged. The selective binding of the biomolecules is one of the most critical factors for SERS detection because the analyte must be present near the enhanced electromagnetic field located at metal nanostructure junctions. The electrostatic attraction of protein A to the silver nanoparticles and the biochemical binding of the Fc region of IgG to protein A provides a clear pathway for the specific detection of the biomolecular species via SERS.

In fact, by using fluorescein-labeled protein A and rhodamine-labeled IgG, it was possible to determine a sequence of the specific adsorption and binding of the biomolecules in striped regions containing silver nanoparticles by following different fluorescent bands (Figure 5). The two different fluorophores selected for proper labeling, fluorescein and rhodamine, have two very different excitation wavelengths and emission wavelengths, which allows for the protein A and IgG adsorption to be separately monitored to verify the presence of each biomolecules. The characteristic emission colors of fluorescein and rhodamine

dx.doi.org/10.1021/la104787w |*Langmuir* 2011, 27, 3198–3205

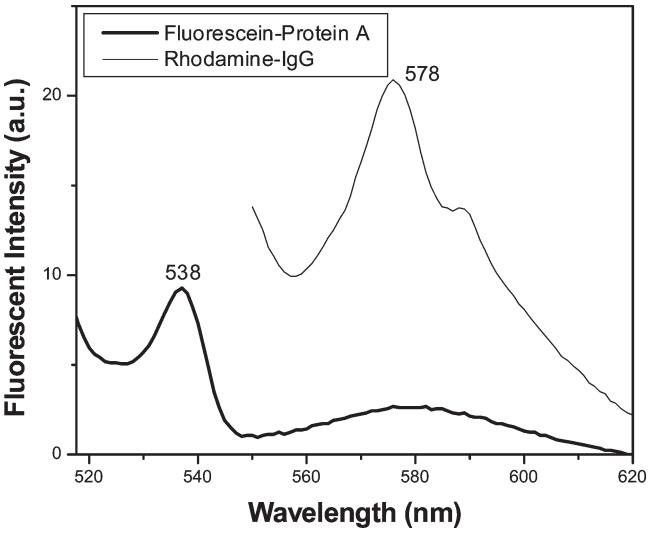

Figure 6. Fluorescent spectra after the adsorption of protein A and IgG on the micropatterned substrate indicating the presence of both fluorophores after final adsorption stage. The 538 nm peak indicates the emission of fluorescein-conjugated protein A obtained at an excitation wavelength of 495 nm, and the 578 nm peak indicates the emission of Rhodamine-conjugated IgG obtained at an excitation wavelength of 550 nm.

are green and red, respectively, as can be revealed by excitation with different wavelengths (see discussion below and corresponding UV−vis spectra in Figure 6).

The nanoparticle micropatterned surface was first exposed to a solution of fluorescein-labeled protein A. The fluorescent microscope image in Figure 5b clearly shows that the fluorescein is present only in regions containing nanoparticles, as confirmed by comparison to the dark field image in Figure 5a. This detection is possible because an excitation wavelength of 495 nm was used, which is the wavelength associated with fluorescein. This result indicates that protein A is selectively binding to the silver nanoparticles on the substrate. This will subsequently allow for specific adsorption of IgG onto the nanoparticles, resulting in the optimum condition for SERS detection of the biomolecules. The fluorescent emission of rhodamine molecules can also be clearly seen using an excitation wavelength of 550 nm following rhodamine-labeled IgG adsorption to the surface (Figure 5c). Both fluorescence images show that the proteins specifically bind in regions containing nanoparticles, meaning that the proteins are in optimal locations on the sample for SERS enhancement.

To ensure that IgG was binding to protein A and not replacing it on the surface, additional measurements were performed. In these measurements, fluorescent spectroscopy was conducted to confirm the presence of both fluorophores on the substrate at two different excitation wavelengths (Figure 6). The presence of two strong bands (corresponding to fluorescein and rhodamine) on the fluorescent spectra of the final micropatterned substrate containing both fluorescein-labeled protein A and rhodamine-labeled IgG confirms the presence of both biomolecules following the final adsorption step. The characteristic fluorescent emission peaks for fluorescein (538 nm) and rhodamine (578 nm) are both present after sequential adsorption with protein A. This indicates that both proteins remain on the surface due to strong tethering between oppositely charged groups. It is speculated that the shouldering that is present on the Rhodamine−IgG curve may be the result of the complex interactions

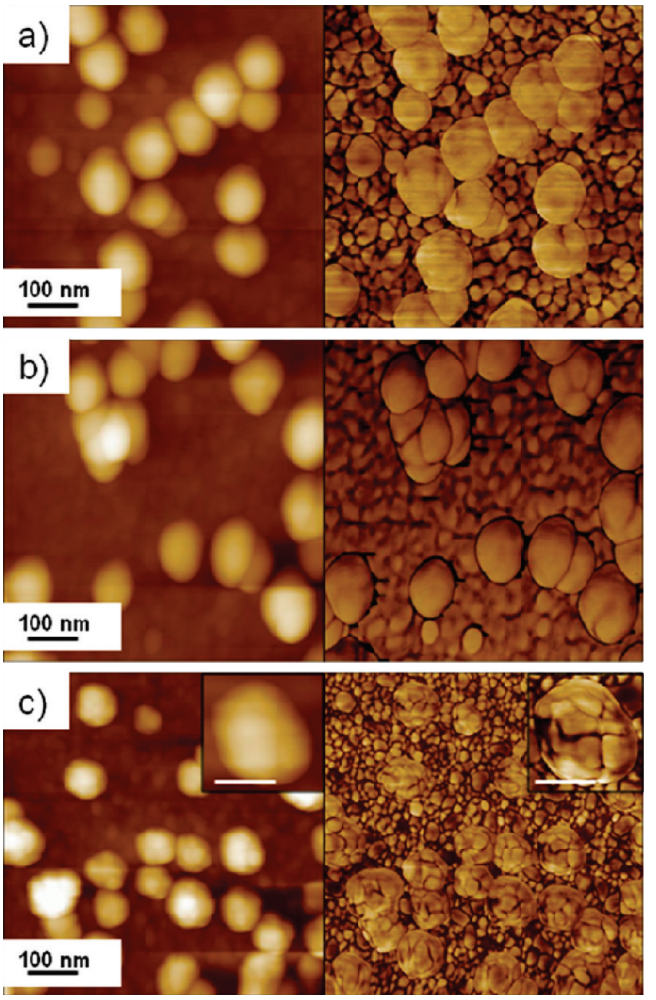

Figure 7. High resolution AFM topographical and phase images of the silver nanoparticle regions of the micropatterned substrate (a) before, (b) after protein A adsorption, and (c) after IgG adsorption. The *z* scale of all images is 80 nm. The scale bar in the single particle inset is 45 nm.

between the fluorophores and proteins present on the substrate. This spectroscopic result shows that both protein A and IgG remained tethered to the silver nanoparticles after the final protein binding sequence and thorough washing cycles (Figure 4, bottom panel).

High resolution AFM images of the micropatterned regions were additionally collected to determine the difference before and after adsorption of protein A and IgG on/between silver nanoparticles (Figure 7). Figure 7a shows the region of the micropatterned substrate before exposure to the biomolecular analytes. Smooth and round silver nanoparticles demonstrate uniform phase response of their surface prior to biomolecule adsorption. Following protein A adsorption on the substrate (Figure 7b) there is little apparent change in the surface of the particles in either the height or phase images. This is likely due to the small size of protein A compared to the silver nanoparticles and the possibility that the protein has collapsed on the surface of the particles as a result of strong electrostatic interactions.

Finally, the high resolution AFM images following IgG adsorption show roughened nanoparticles, confirming that multiple small globules are bound to the surface of the nanoparticles after adsorption with several patches clearly visible on each

dx.doi.org/10.1021/la104787w |*Langmuir* 2011, 27, 3198–3205

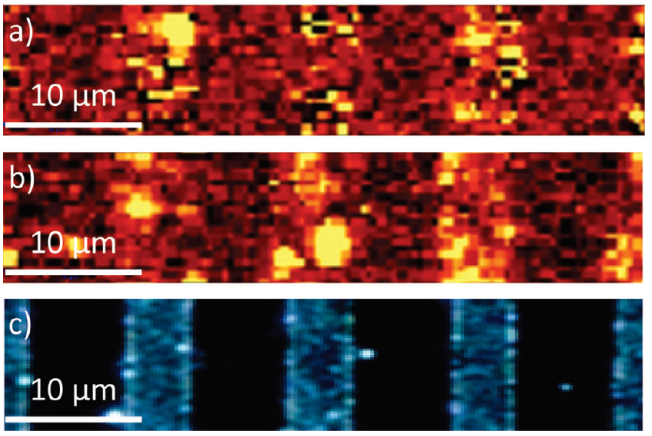

Figure 8. SERS mapping of the substrate following (a) protein A and (b) IgG adsorption and (c) an optical image of the substrate to indicate the location of the striped regions in the SERS maps. The peak mapped for protein A was 1507 cm^{-1}, indicative of lysine found in protein A, and the peak mapped for IgG was 1649 cm^{-1}, indicative of the tryptophan v ring stretching.

nanoparticle (Figure 7c). The drastic change in both the height and the phase image indicates that IgG is binding to the surfaces of the silver nanoparticles and not just adsorbed on surrounding surface areas. The binding of the biomolecules in close proximity to or on the surface of the nanoparticles is necessary for SERS enhancement to occur. These images indicate that IgG readily binds to the nanoparticles even with the modest concentration (5×10^{-7} M) and short exposure time (30 s) of the IgG used in these experiments.

When concentration and exposure time were increased, multiple layers and complete coverage of the silver nanoparticles on the substrate was observed, which completely masked initial domain morphology. The typical Y-shape of IgG is not always visible using AFM because the biomolecule does not always exists in this state as a bound molecule.[49] Globular conformations of bound IgG on surfaces similar to the bound protein shown in Figure 7c have been previously shown.[50] The obvious change in the surface topography of the regions of the micropatterned sample containing nanoparticles combined with the previously discussed fluorescence studies clearly indicates that the biomolecular analytes in this study are bound to silver nanoparticles.

Raman Mapping of Adsorbed Biomolecules. Raman mapping visualized the selective surface distribution of the adsorbed biomolecules (Figure 8). The significant enhancement of the Raman signal of protein A and IgG on SERS substrate is clearly shown in the mapping images. The stripes from the micropatterned substrate can be seen in the mapping images. The peaks of highest intensity in the Raman spectra of the two biomolecules used in this study were mapped across the substrate surface. The peak mapped for protein A (Figure 8a) was the 1507 cm^{-1} peak and the peak mapped for IgG (Figure 8b) was the 1649 cm^{-1} peak. Figure 8c shows an optical microscope image concurrently obtained for the patterned substrate to guide to the location of the striped regions in the Raman maps. The regions of the stripes shown in the figure that do not exhibit a complete and uniform response are due to the low concentration of protein A and IgG used in this test.

The low concentrations of protein solutions used in this study and the very low exposure time (30 s) to the substrate prevented clogging the micropatterned substrate and the formation of

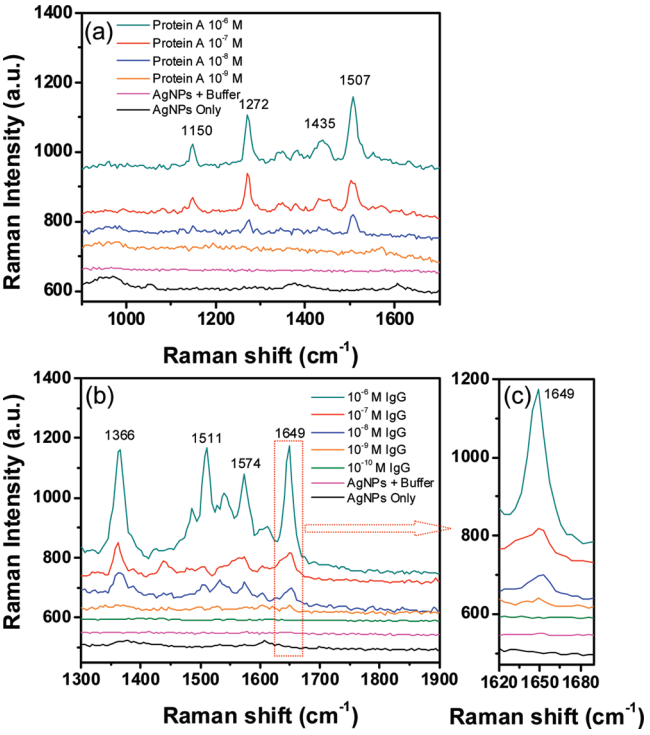

Figure 9. SERS spectra of (a) protein A and (b) IgG on the silver nanoparticle substrate compared to references of the neat micropatterned substrate and the substrate following buffer exposure. The characteristic peak of IgG at 1649 cm^{-1}, which is used for limit of detection measurements, is shown at larger scale (c).

relatively thick biofilms with an incomplete monolayer of biomolecules formed on the surface of the nanoparticle-decorated areas. Indeed, cross sections of AFM images show that the average nanoparticle height increased from 33 ± 4 to 38 ± 3 nm following protein A and IgG adsorption, indicating that only about 4 nm of IgG could have adsorbed on the nanoparticle surface, which is less that the diameter of the native biomolecules. Moreover, independent measurements with ellipsometry also confirmed that the increase of the effective thickness associated with adsorbed protein was less than 5 nm, thus additionally confirming low surface coverage with biomolecules. When large amounts of IgG were used, the SERS intensity reached a point at which there was no change in intensity on the patterned regions. The substrate was designed for the trace detection of biomolecules so there was limited testing at higher concentrations.

Limit of Detection of Protein A and IgG. A limit of detection study of protein A and IgG was also conducted using the micropatterned SERS substrate to demonstrate that fast, label-free, and trace detection is possible with this substrate (Figure 9). The limit of detection of the substrate was determined on the basis of the principle that the peak intensity of the analyte must be greater than background variation by more than a factor of 3.[11] Spectra from the SERS substrate were taken in reflection mode after protein A adsorption and subsequently after IgG adsorption on the surface.

For the IgG limit of detection, the substrate was exposed to a protein A solution of 10^{-8} M to prevent the very intense peaks of protein A from interfering with IgG detection. The peak assignment in the SERS spectrum of protein A is proposed on the basis of knowledge of the amino acid sequence of protein A and literature data on characteristic vibrations for different amino

dx.doi.org/10.1021/la104787w |*Langmuir* 2011, 27, 3198–3205

acids (Figure 9a).[51] The spectral peaks of 1150 and 1507 cm^{-1} can be attributed to lysine and the peak at 1272 cm^{-1} can be assigned to glutamine and asparagine. These three amino acids exist in high concentration in protein A. As a result of the positive charge of lysine, it is thought that this residue of protein A exists in closest proximity to the negatively charged SERS hot spots leading to a greater contribution to the overall spectrum of protein A from lysine than other residues present.

The characteristic SERS bands of IgG can be also found following IgG adsorption (Figure 9b,c). Raman peaks at 1366, 1511, 1574, and 1649 cm^{-1} are indicative of the tryptophan v ring stretching and the peaks at 1511 and 1574 cm^{-1} also indicate the tyrosine v ring stretching, which are both the characteristic Raman-active amino acid sequences of IgG.[25] The peak at 1649 cm^{-1} is the most consistent peak seen in the IgG spectra but seems to be shifted slightly in comparison to literature values. This may be a result of the presence of protein A as an intermediate biding agent, as well as the fact that residues that include α-helical amide I groups from IgG may be bound close to the silver nanoparticle hot spots than other parts of the IgG molecule.[52] The SERS enhancement of protein A and IgG allows for accurate detection of the presence of these biomolecules while the micropatterned surface provides a platform that specifically binds protein A and IgG in silver nanoparticle hot spot regions. The limit of detection was measured for a stepwise decreasing of protein solutions concentration to 100 fM (Figure 9). For protein A the low limit of detection was determined to be around 5 nM, as estimated from peak at 1507 cm^{-1} in accordance with a general procedure described above for IgG protein.

For IgG protein, the Raman peak at 1649 cm^{-1} was used to follow the adsorption process with a very intense peak observed at 10^{-6} M concentration and only random background observed for 100 fM solution. Increasing the concentration to 10 nM results in the appearance of a strong peak at 1649 cm^{-1}. The peak is less intense but exceeds the random background level by a factor of 4 at 1 nM and thus gives the evaluation of the lowest detection limit achievable here as well below 1 nM (close to 500 fM). Such a very low limit of detection of nonlabeled IgG solution is within common limits of detection of these biomolecules reported in literature with different methods all of which require additional labeling procedure.[53]

CONCLUSIONS

In conclusion, we demonstrated that a nanoengineered substrate composed of micropatterned metal nanoparticles can be exploited for the SERS detection of the known bioanalytes, protein A and human immunoglobulin G (IgG). The amine-terminated nanocoating prevents the surface adsorption of positively charged protein A across the surface except the selective patterned regions containing negatively charged silver nanoparticles. In turn, protein A facilitates subsequent selective adsorption of IgG on predetermined regions. SERS detection was made possible by the high concentration of hot spots, which occurred between the densely packed silver nanoparticles.

This design possesses advantages over current methods such as ELISA, SPR, and FRET which include label-free and fast detection using a simple and cost-effective substrate fabrication technique. This approach might provide accurate, sensitive, and more selective detection of protein A and IgG than current protein detection methods with the lowest limit of detection for IgG protein solution of below 1 nM, which is comparable to the sensitivity of traditional optical biosensing methods. An additional clear advantage of this highly sensitive SERS method on an engineered substrate is the speed of detection and simple substrate preparation. Moreover, this method does not require several binding and purification steps as in ELISA which can take hours to complete. Simple exposure of the substrate to the biomolecule solution allows for rapid SERS detection in less than several minutes. This method is also cost-effective in that fluorescently labeled proteins are not required for detection.

The robust and label-free detection of the positively charged protein A is based on electrostatically driven selective bounding to regions containing the negatively charged silver nanoparticle hot spots and thus can be applied to a wide variety of proteins properly (positively, for this design) charged. This method has the potential to provide a simple, fast, label-free, selective, and economical substrate for the Raman mapping of a wide range of adsorbed biomolecules. We suggest that this method also could be utilized for the detection of low concentration protein solutions in clinical, forensic, industrial, and environmental laboratories.

AUTHOR INFORMATION

Corresponding Author

*E-mail: vladimir@mse.gatech.edu.

ACKNOWLEDGMENT

We thank NSF CBET-0930781 for funding this research and the NDSEG Fellowship Program for Z.A.C. and K.D.A.

REFERENCES

(1) Siqueira, J. R.; Caseli, L.; Crespilho, F. N.; Zucolotto, V.; Oliveira, O. N. *Biosens. Bioelectron.* **2009**, *25*, 1254–1263.
(2) Engvall, E.; Perlman, P. *Immunochemistry* **1971**, *8*, 871–874.
(3) Homola, J. *Anal. Bioanal. Chem.* **2003**, *377*, 528–539.
(4) Weiss, S. *Science* **1999**, *283*, 1676–1683.
(5) Nie, S. M.; Emory, S. R. *Science* **1997**, *275*, 1102–1106.
(6) Kneipp, K; Wang, Y.; Kneipp, H.; Perelman, L. T.; Itskan, I.; Dasari, R.; Feld, M. S. *Phys. Rev. Lett.* **1997**, *78*, 1667–1670.
(7) Ko, H.; Singamaneni, S.; Tsukruk, V. V. *Small* **2008**, *4*, 1576–1599.
(8) Larsson, M.; Lindgren, J. *J. Raman Spectrosc.* **2005**, *36*, 394–399.
(9) Pavel, I.; McCarney, E.; Elkhaled, A.; Morrill, A.; Plaxco, K.; Moskovits, M. *J. Phys. Chem. C* **2008**, *112*, 4880–4883.
(10) Cho, H.; Lee, B.; Liu, G. L.; Agarwal, A.; Lee, L. P. *Lab Chip* **2009**, *9*, 3360–3363.
(11) Ko, H.; Chang, S.; Tsukruk, V. V. *ACS Nano* **2009**, *3*, 181–188.
(12) Kneipp, K.; Kneipp, H.; Kneipp, J. *Acc. Chem. Rev.* **2006**, *39*, 443–450.
(13) Thaxton, C. S.; Elghanian, R.; Thomas, A. D.; Stoeva, S. I.; Lee, J. S.; Smith, N. D.; Schaeffer, A. J.; Klocker, H.; Horninger, W.; Bartsch, G.; Mirkin, C. A. *Proc. Natl. Acad. Sci. U. S. A.* **2009**, *106* (44), 18437–18442.
(14) Freeman, R. G.; Grabar, K. C.; Allison, K. J.; Bright, R. M.; Davis, J. A.; Guthrie, A. P.; Hommer, M. B.; Jackson, M. A.; Smith, P. C.; Walter, D. G.; Natan, M. J. *Science* **1995**, *267*, 1629–1632.
(15) Wang, Z.; Pan, S.; Krauss, T. D.; Du, H.; Rothberg, L. J. *Proc. Natl. Acad. Sci. U. S. A.* **2003**, *100*, 8638–8643.
(16) Hulteen, J. C.; Treichel, D. A.; Smith, M. T.; Duval, M. L.; Jensen, T. R.; Van Duyne, R. P. *J. Phys. Chem. B* **1999**, *103*, 3854–3863.
(17) Gunawidjaja, R.; Peleshanko, S.; Ko, H.; Tsukruk, V. V. *Adv. Mater.* **2008**, *20*, 1544–1549.

(18) Qin, L.; Zhou, S.; Xue, C.; Atkinson, A.; Schatz, G. C.; Mirkin, C. A. *Proc. Natl. Acad. Sci. U. S. A.* **2006**, *103*, 13300–13303.
(19) Gobin, A. M.; Lee, M. H.; Halas, N. J.; James, W. D.; Drezek, R. A.; West, J. L. *Nano Lett.* **2007**, *7*, 1929–1964.
(20) Ko, H.; Tsukruk, V. V. *Small* **2008**, *4*, 1980–1984.
(21) Campbell, N. A.; Reece, J. B.; Mitchell, L. G. *Biology*, 5th ed.; Benjamin/Cummings: Menlo Park, CA, 1999,; p 853.
(22) Alberts, B.; Johnson, A.; Lewis, J.; Raff, M.; Roberts, K.; Walter, P. *Molecular Biology of the Cell*, 4th ed.; Garland Science: New York, 2003; p 1376.
(23) Rosi, N. L.; Mirkin, C. A. *Chem. Rev.* **2005**, *105*, 1547–1562.
(24) Stewart, S.; Fredericks, P. M. *Spectrochim. Acta, Part A* **1999**, *55*, 1615–1640.
(25) Grabbe, E. S.; Buck, R. P. *J. Am. Chem. Soc.* **1989**, *111*, 8362–8366.
(26) Moskovits, M.; Suh, J. S. *J. Phys. Chem.* **1984**, *88*, 5526–5530.
(27) Moskovits, M. *Rev. Mod. Phys.* **1985**, *57*, 783–826.
(28) Kneipp, K. *Phys. Today* **2007**, *16*, 40–46.
(29) Camden, J. P.; Dieringer, J. A.; Zhao, J.; Van Duyne, R. P. *Acc. Chem. Res.* **2008**, *41* (12), 1653–1661.
(30) Ko, H.; Tsukruk, V. V. *NanoLett.* **2006**, *6*, 1443–1448.
(31) Xia, Y.; Whitesides, G. M. *Annu. Rev. Mater. Sci.* **1998**, *28*, 153–184.
(32) (a) Ko, H.; Jiang, C.; Tsukruk, V. V. *Chem. Mater.* **2005**, *17*, 5489–5497. (b) Jiang, C.; Markutsya, S.; Shulha, H.; Tsukruk, V. V. *Adv. Mater.* **2005**, *17*, 1669–1673.
(33) Muramatsu, H.; Dicks, J. M.; Tamiya, E.; Karube, I. *Anal. Chem.* **1987**, *59*, 2760–2763.
(34) Sato-Berrú, R.; Redón, R.; Vázquez-Olmos, A.; Saniger, J. M. *J. Raman Spectrosc.* **2009**, *40*, 376–380.
(35) Kharlampieva, E.; Kozlovskaya, V.; Chan, J.; Ankner, J. F.; Tsukruk, V. V. *Langmuir* **2009**, *25*, 14017–14024.
(36) Tsukruk, V. V.; Bliznyuk, V. N. *Langmuir* **1998**, *14*, 446–455.
(37) Jiang, C.; Markutsya, S.; Pikus, Y.; Tsukruk, V. V. *Nat. Mater.* **2004**, *3*, 721–728.
(38) Jiang, C.; Markutsya, S.; Tsukruk, V. V. *Adv. Mater.* **2004**, *16*, 157–161.
(39) Jiang, C.; Markutsya, S.; Shulha, H.; Tsukruk, V. V. *Adv. Mater.* **2005**, *17*, 1669–1673.
(40) Jiang, C.; Tsukruk, V. V. *Soft Matter* **2005**, *1*, 334–337.
(41) Tsukruk, V. V. *Rubber Chem. Technol.* **1997**, *70*, 430–467.
(42) McConney, M. E.; Singamaneni, S.; Tsukruk, V. V. *Polym. Rev.* **2010**, *50*, 235–286.
(43) Singamaneni, S.; Gupta, M.; Yang, R.; Tomczak, M. M.; Naik, R. R.; Wang, Z. L.; Tsukruk, V. V. *ACS Nano* **2009**, *3*, 2593–2600.
(44) Van Hoonakcer, A.; Englebienne, P. *Curr. Nanosci.* **2006**, *2*, 359–371.
(45) Ghosh, S. K.; Pal, T. *Chem. Rev.* **2007**, *107*, 4797–4862.
(46) Jain, P. K.; El-Sayed, M. A. *Nano Lett.* **2007**, *7*, 2854–2858.
(47) Jiang, C.; Markutsya, S.; Tsukruk, V. V. *Langmuir.* **2004**, *20*, 882–890.
(48) Wrosek, K.; Gramblicka, M.; Tothova, D.; Antosova, M.; Polakovic, M. *Chem. Pap.* **2010**, *64*, 461–468.
(49) Han, W.; Mou, J.; Sheng, J.; Yang, J.; Shao, Z. *Biochemistry* **1995**, *34*, 8215–8220.
(50) San Paulo, A.; Garcia, R. *Biophys. J.* **2000**, *78*, 1599–1605.
(51) Guss, B.; Leander, K.; Hellman, U.; Uhlén, M.; Sjöquist, J.; Lindberg, M. *Eur. J. Biochem.* **1985**, *153*, 579–585.
(52) Dou, X.; Yamaguchi, Y.; Yamamoto, H.; Doi, S.; Ozaki, Y. *J. Raman Spectrosc.* **1998**, *29*, 739–742.
(53) Chon, H.; Lim, C.; Ha, S. M.; Ahn, Y.; Lee, E. K.; Chang, S. I.; Seong, G. H.; Choo, J. *Anal. Chem.* **2010**, *82*, 5290–5295.